

COMPARISON OF VEGETATION ANOMALIES TO EL NIÑO-SOUTHERN OSCILLATION IN CHINA AND AUSTRALIA

Cong Wang¹

¹Key Laboratory for Geographical Process Analysis & Simulation of Hubei Province/ School of Urban and Environmental Sciences, Central China Normal University, Wuhan 430079, China - wangcong@ccnu.edu.cn

Commission III, WG III /10

KEY WORDS: vegetation anomaly, El Niño-Southern Oscillation, Central-Pacific type, Eastern-Pacific type, China, Australia.

ABSTRACT:

The El Niño-Southern Oscillation (ENSO), as one of the main factors driving extreme climate events, exerts a major influence on interannual climate variability around the world. However, ENSO effects on vegetation, especially regarding the extent, intensity, direction, are not well understood. Here, we characterize and compare the variability in vegetation response to ENSO across China and Australia and explore their underlying mechanisms. Results show that the spatial extent of ENSO-sensitive vegetation differed between China and Australia and across land cover types. For both China and Australia, the intensity and direction of vegetation anomalies were closely related to the type of ENSO events. In particular, vegetation anomalies to the Central-Pacific (CP) type ENSO events were stronger than that to the Eastern-Pacific (EP) type events of the same intensity and generally responded in an opposite way, resulting from different controls of CP-type and EP-type ENSO on precipitation and temperature. Our findings highlight the diverse response of vegetation triggered by different types of ENSO in China and Australia, which can improve our understanding of ENSO impacts on ecosystems in the northern and southern hemispheres.

1. INTRODUCTION

The El Niño-Southern Oscillation (ENSO), a recurring oscillation of coupled ocean-atmosphere dynamics in the eastern-to-central equatorial Pacific, has been recognized as one of the primary sources of interannual climate variability across the globe (McPhaden et al., 2006). In addition to neutral conditions, there are two distinct phases: warmer (El Niño) and colder (La Niña) ocean events. These phases lead to a redistribution of precipitation and temperature patterns by affecting atmospheric circulation (Cai et al., 2011; Huang et al., 2015; Yang et al., 2018). During El Niño years, warmer and drier conditions are experienced throughout many regions of the globe, especially tropical regions. Cooler, wetter conditions prevail in many regions during La Niña years (Hao et al., 2018).

Traditionally El Niño/ La Niña were referred to as Eastern-Pacific (EP) events associated with a maximum Sea Surface Temperature Anomaly (SSTA) in the eastern equatorial Pacific. In recent years, a Central-Pacific (CP) event, in which the SSTA shift to the central equatorial Pacific, has been widely discussed (Ashok et al., 2007; Kao et al., 2009; Kim et al., 2012; Yu et al., 2011). Although CP events were rarely observed prior to the 1980s, they have occurred frequently during the past three decades (Lee and McPhaden, 2010), likely in response to weakened equatorial easterlies observed over the central Pacific (Ashok et al., 2007) or increased temperatures attributed to climate change (Yeh et al., 2009). The active convection area for CP El Niño/ La Niña events develops west of the convection area associated with EP El Niño/ La Niña events, forming two anomalous Walker circulation circles over the equatorial Pacific. This circulation change may result in an influence on climate anomalies opposite to that of EP ENSO events (Kao et al., 2009; Kim et al., 2012; Yu et al., 2011). For example, it has been shown that southern China experiences increased rainfall during

the decaying spring and summer of EP El Niño events but reduced rainfall during those same seasons during CP El Niño events (Feng and Li, 2011).

Structure and function of vegetated ecosystems have been significantly affected by climate variability induced by ENSO, at regional scales (Vicente-Serrano et al., 2006; Walther et al., 2002; Xu et al., 2011), especially in Australia (Ma et al., 2015; Xie et al., 2019), Africa (Hao et al., 2020; Propastin et al., 2009), and North America (Dannenberg et al., 2015; Flanagan and Adkinson, 2011; McCabe et al., 2012). For example, ecosystems in eastern and northern Australia (especially semi-arid ecosystems) have been shown to be sensitive to La Niña events (Cai et al., 2011; Poulter et al., 2014; Xie et al., 2019; Zhang et al., 2017), in which the predominate effect is related to precipitation anomalies. However, ecosystem responses in China and other regions indirectly affected by ENSO through teleconnections are complex and not well understood (Barriopedro et al., 2012). Moreover, the timing, phase, and duration of ENSO events remain largely uncertain, especially since climate change exacerbates this uncertainty (Collins et al., 2010; Wang et al., 2019; Yuan et al., 2020). This combination of complexity in ecosystem response and uncertainty surrounding ENSO makes it difficult to understand how vegetation will respond to ENSO and which mechanisms will drive these changes.

In this study, we characterize and compare the variability in vegetation response to ENSO from 1982 to 2017 across China and Australia, both of which are climate change research hotspots (Liu et al., 2019; Ma et al., 2015; Poulter et al., 2014; Zhu et al., 2016). We quantify the extent, intensity, and direction of vegetation responses to ENSO, and explored the underlying mechanisms driving changes in those responses by investigating linkages between ENSO, climate, and vegetation.

This investigation improves our understanding of vegetation variability response associated with ENSO events in the northern and southern hemispheres.

2. DATA AND METHOD

2.1 Identification of ENSO Event Occurrence and Type

ENSO indices were downloaded from the National Oceanic and Atmospheric Administration (NOAA) Earth System Research Laboratory (https://www.esrl.noaa.gov/psd/gcos_wgsp/Timeseries) for the Niño 3 region (NINO 3 index; 5°S~5°N, 150°W~90°W), Niño 3.4 region (5°N~5°S, 170°W~120°W), and Niño 4 region (NINO 4 Index; 5°S~5°N, 160°E~150°W). The average value of SSTA over the Niño 3 region (NINO 3 Index) and Niño 4 region (NINO 4 index) were combined to distinguish between EP and CP type events using the criteria specified by Ren and Jin (2011) from 1982 to 2017. The average value of SSTA over the Niño 3.4 region (NINO 3.4 index) was used to identify El Niño/La Niña events, which are defined as a time period when five consecutive SSTA values were greater than 0.5 °C or less than -0.5 °C.

2.2 Satellite Data and Pre-processing

2.2.1 Vegetation Datasets: We utilized spatio-temporally contiguous GLASS LAI data (Global Land Surface Leaf Area Index Product) at 0.05° and 8-day resolution from 1982 to 2017 as a proxy for vegetation (<http://glass-product.bnu.edu.cn/introduction/LAI.html>). The 8-daily LAI was aggregated to a monthly composite to match the temporal interval of the ENSO indices. To avoid spurious correlations resulting from trends in the data, LAI data were linearly detrended by subtracting the long-term linear trend, obtained by using a least squares regression fit on the original time series (Ma et al., 2015; Zhu et al., 2017). Since the GLASS LAI in 1982~2000 and 2001~2017 were obtained based from AVHRR and MODIS surface reflectance data respectively, we detrended both LAI time series to eliminate any influence resulting from using different sensors. Standardized anomalies were calculated by dividing anomalies by the standard deviation based on z-score function (Ma et al., 2015; Flanagan and Adkinson, 2011; Xie et al., 2019). Because low LAI values tend to be affected by environmental noise with high uncertainty, we excluded those pixels where the annual average LAI was less than 0.1.

2.2.2 Climate Datasets and Land Cover Type: Temperature and precipitation observations were obtained from the ERA-Interim global reanalysis data provided by the European Centre for Medium-Range Weather Forecasts (ECMWF) at 0.125° and 6-hourly resolution (<https://apps.ecmwf.int/datasets/data>). We aggregated the original climate datasets to a monthly time scale at 0.05° resolution to match the resolution of the vegetation datasets. Standardized anomalies were then calculated using the method described in Section 2.2.1. Land cover type was identified using the MCD12C1 V005 product at 0.05° resolution.

2.3 Sensitivity Assessment of Vegetation to ENSO Events

Statistical analysis was used to investigate the relationship between vegetation variability and ENSO. Since the extent of ENSO-affected areas is not consistent across ENSO events and the duration of each ENSO event is variable, Pearson's Chi-

Square test, which evaluates the correlation between two disordered categorical variables, was applied to identify those areas where variability in vegetation response was sensitive to ENSO events (Lv et al., 2012). The Pearson's Chi-Square is calculated as follows:

$$\chi^2 = \frac{(m - n * p_b)^2}{n * p_b * (1 - p_b)} \quad (1)$$

Where n is the number of months when El Niño/La Niña events occurred; m is the number of months when extensive vegetation anomalies (LAI z-score > 1 or < -1) occurred during the El Niño/La Niña events; and p_b is the probability that the vegetation experiences extensive variation under normal conditions.

Although Lv et al. (2012) employed the Chi-Square test to identify ENSO-sensitive areas in China, this test failed to distinguish whether vegetation anomalies occurred during the ENSO events or not, since χ^2 can only be positive. We improved upon this approach by adding an additional condition as follows:

$$m - n * p_b > 0 \quad (2)$$

When (1) χ^2 reaches the threshold χ_{α}^2 ($\alpha=0.05$ and degree of freedom is 1) and (2) the condition is met, vegetation in this pixel is considered sensitive to ENSO events.

2.4 Major Climatic Factors Driving Vegetation Growth

To examine time-lag effects of vegetation responses to different climatic factors (Wu et al., 2015), a cross correlation analysis was adopted to explore the relationship between vegetation and the temperature and precipitation anomalies induced by ENSO as follows (Xie et al., 2019):

$$cr = \frac{\sum_i^k [(x(i) - mx) * (y(i-l) - my)]}{\sqrt{\sum_i^k (x(i) - mx)^2} \sqrt{\sum_i^k (y(i-l) - my)^2}} \quad (3)$$

where cr is the cross correlation coefficient between x and y , x is the vegetation time series and y is either temperature or precipitation time series, mx and my are the means of x and y time series, respectively. k is the total number of months, l represents the time lag in months. As the influence of ENSO on vegetation response can span years, time lags from -12 to 12 months were considered in the analysis.

3. RESULTS

3.1 Extent of ENSO-Sensitive Vegetation Areas

The spatial extent of ENSO-sensitive vegetation differed in China and Australia and varied with land cover (Figure 1). El Niño-sensitive areas were concentrated mainly in southern China, where the main vegetation types were savannas and mixed forests. However, La Niña -sensitive areas were mainly distributed in the croplands of central China and the grasslands

in northern Inner Mongolia as well as on the northern Tibetan Plateau. La Niña-sensitive areas were slightly larger than El Niño-sensitive areas in China (20.9 % and 14.4% respectively). Only small proportions of vegetation (< 5%) in China were sensitive to both El Niño and La Niña events.

In contrast, most vegetation in Australia was not sensitive to El Niño events, with results showing a scattered distribution, while larger proportion of the vegetated area was affected by La Niña than by El Niño events (57.6% vs. 8.5%). La Niña-sensitive areas were concentrated in northern and eastern Australia, which is consistent with previous studies (Cai et al., 2011; Xie et al., 2019). Moreover, areas with vegetation sensitive to both El Niño and La Niña were mainly concentrated in the woody savannas of northern Australia. In Australia, shrublands (43.2% of the vegetated area) comprised the largest share of ENSO-sensitive areas, followed by savannas (5.0%), woody savannas (4.9%) and grasslands (3.1%).

Overall, the sensitivity of vegetation to different phases of ENSO differed spatially and varied by vegetation cover type. The distribution of ENSO-sensitive vegetation areas in China are more discrete and scattered than that of Australia as a result of the complex distribution of vegetation, climate, topography in China as well as human activities and their complicated interactions, as discussed in section 4.

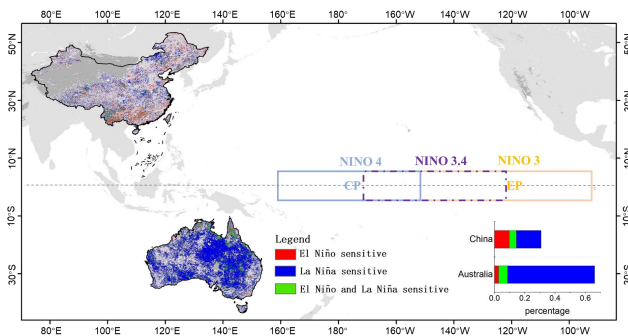


Figure 1. The distribution of ENSO-sensitive vegetation areas.

3.2 Intensity and Direction of Vegetation Responses to Different Types of ENSO

In this study, we define the intensity and direction of vegetation responses to ENSO by the absolute value and sign of the maximum vegetation anomalies respectively during each ENSO event. Then statistics analysis was conducted based on the pixels that were sensitive to ENSO.

In general, vegetation anomalies in China and Australia increased as the intensity of ENSO events increased (Figure 2). Vegetation responses to El Niño events in China were stronger than those in Australia (Figure 2a), while vegetation anomalies associated with La Niña events were stronger in Australia than in China, especially for CP types (Figure 2b). However, for both China and Australia, vegetation response was more sensitive to La Niña events than to El Niño events when the slopes of the El Niño and La Niña event lines were compared for the same distribution type (Figure 2 a and b). Although strong ENSO events were almost EP type events, vegetation response anomalies to CP-type ENSO events were larger than those to EP events for the same intensity across both China and Australia.

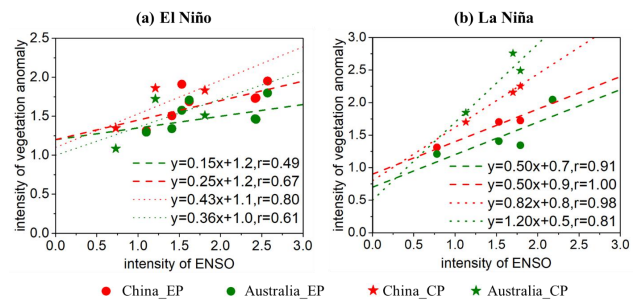


Figure 2. The relationship between the intensity of vegetation anomalies and different types of ENSO. (a) El Niño; (b) La Niña. Red and green dots indicate EP type events for China and Australia, respectively, while stars indicate CP type events. The dashed and dotted lines indicate linear regressions between the intensity of vegetation anomalies and EP-type and CP-type ENSO events, respectively.

Previous studies have shown that vegetation in Australia generally has a significant negative correlation with the ENSO index (Zhang et al., 2017; Zhang et al., 2019), that is, Australian vegetation tends to develop negative anomalies during El Niño events and positive anomalies during La Niña events. Our results reveal that there is a lot of uncertainty in the direction of vegetation anomaly associated with an ENSO event. Even with the same event type (e.g., EP-El Niño), vegetation often responds quite differently (Figure 3). In spite of this, we discovered that the direction of vegetation anomalies may have a certain statistical relationship with ENSO distribution. Vegetation in Australia tends to have increased LAI anomalies (positive direction) during CP-type La Niña events, but decreased LAI anomalies (negative direction) during EP-type La Niña events. In China, CP-type El Niño events tend to trigger negative vegetation anomalies, while EP-type El Niño events may result in either positive or negative vegetation anomalies.

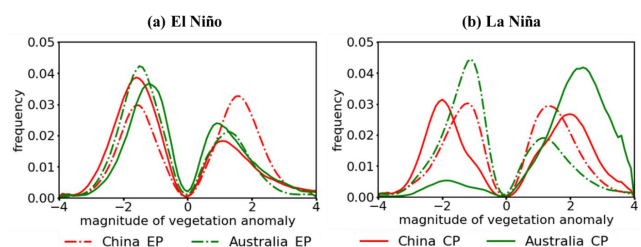


Figure 3. Frequency distribution of magnitude of vegetation anomalies during different ENSO conditions associated with (a) El Niño and (b) La Niña events of type EP (dashdotted) and CP (solid).

3.3 Climate Drivers for Vegetation Anomalies to Different Types of ENSO

Spatially, vegetation in China and Australia showed a variety of responses to the different ENSO types (Figures 4 and 5), which is consistent with the findings reported in Section 3.2.

Throughout most of Australia, and especially in the eastern areas, vegetation anomalies have a positive correlation with precipitation anomalies and a negative correlation with

temperature anomalies. During CP-type La Niña events, increased precipitation and decreased temperature consistently lead to positive vegetation anomalies (Figure 4). In contrast, EP-type La Niña events have a weaker, more heterogeneous effect on precipitation and temperature in Australia. Increased precipitation and decreased temperature occurred in the northeastern coastal areas while northern and mid-western Australia experienced decreased precipitation and increased temperature, leading to negative anomalies for vegetation in these areas during EP-type La Niña events.

In comparison, vegetation response to ENSO events were spatially heterogeneous in China (Figure 4-5), driven by temporal and spatial variation in both precipitation and temperature. In general, vegetation in China exhibited an opposite response, with negative anomalies during CP-type El Niño events and positive anomalies during EP-type El Niño events (Figure 5). During La Niña events, however, the Qinghai-Tibet Plateau and the northwestern of Yunnan Province were the only areas to show a different response, in which the majority of vegetation anomalies were driven by weak precipitation and high temperature in winter. It should be noted that there may still be uncertainty surrounding the direction of vegetation response for the same ENSO type, especially in China, which may not appear in a multi-year calculation, being offset by other responses.

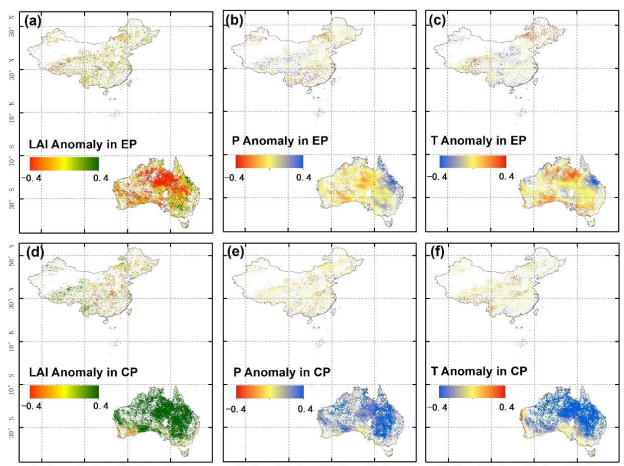


Figure 4. Multi-year average vegetation (LAI), precipitation (P), and temperature (T) anomalies during La Niña events for China and Australia. (a)-(c) Mean anomalies during EP La Niña events; (d)-(f) Mean anomalies during CP La Niña events.

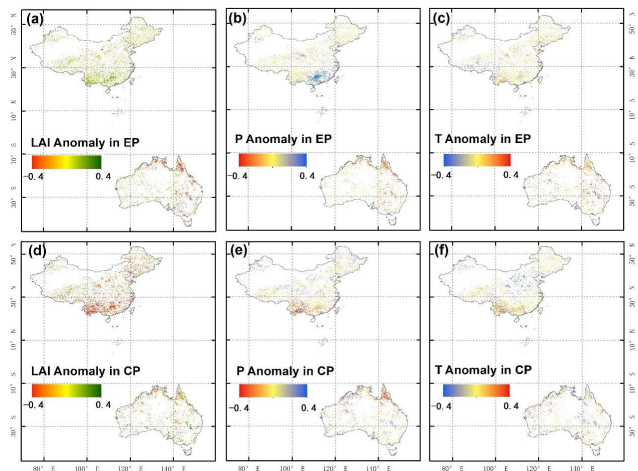


Figure 5. Multi-year average vegetation (LAI), precipitation (P), and temperature (T) anomalies during El Niño events for China and Australia. (a)-(c) Mean anomalies during EP El Niño events; (d)-(f) Mean anomalies during CP El Niño events.

4. DISCUSSIONS

This study revealed that the type of ENSO is an important factor resulting in the intensity and direction of vegetation anomalies for China and Australia. We found that the vegetation responses to the CP type ENSO events were stronger than those to the EP type events of the same intensity in both China and Australia. We infer from this that the impacts of CP-type events on climate anomalies are greater than those of EP-type events as CP-type ENSO conditions (in Central-Pacific) develop closer to China and Australia. Preceding studies have demonstrated that the two distribution types of ENSO are fundamentally different in terms of evolution characteristics, occurrence mechanisms, and climate impacts (Kao and Yu, 2009; Kim and Yu, 2012; Yu et al., 2011; Yu and Kim, 2010). Vegetation, especially in Australia, responded in an opposite manner as a result of the opposing impact of CP and EP ENSO events on precipitation and temperature. These findings highlight the diverse response of vegetation triggered by the location of ENSO development, improving our understanding of ENSO impacts to ecosystems.

We mapped El Niño-sensitive areas and La Niña-sensitive areas for China and Australia from 1982 to 2017, analyzing them using an improved Chi-Square test. We excluded vegetation anomalies during ENSO-neutral periods thereby considering only vegetation response anomalies during ENSO events, but it should be noted that other periodic atmospheric oscillations (such as the Indian Ocean dipole, Arctic Oscillation) and human activities also affect vegetation anomalies and are not accounted for in this study (Xie et al., 2019). We further found that the vegetation response to opposing ENSO phases differed in the same area. La Niña-sensitive areas in Australia were much larger than the El Niño-sensitive areas. Although El Niño likely exerts an influence on Australian wildfires, due to the development of extreme hot and dry conditions under El Niño (Dowdy, 2018; Mariani et al., 2016; Williamson et al., 2016), the fire frequency and burned area varied greatly in Australia during different El Niño events, making it difficult to characterize such areas as being El Niño-sensitive areas.

In comparison, vegetation in China responds in an opposite manner and with weaker intensity. Previous studies have shown that the ENSO impacts on ecosystems differ in northern and southern hemispheres (Zhang et al., 2017; Zhu et al., 2017) as well as regional scales (Zhang et al., 2019), which support our results. Moreover, vegetation anomalies to ENSO events have distinct spatial heterogeneity in China. Possible reasons include: 1) the vegetated landscape has a complex and mosaic distribution pattern developed by fragmentation and intersection of various vegetation patches (Su et al., 2020), resulting in scattered distribution of ENSO-sensitive areas; 2) the spatial distribution of climate, topography, and human activities varies, also leading to heterogeneous spatial patterns in vegetation responses to ENSO; 3) land cover, especially agriculture and urbanization, have changed greatly from 1982 to 2017 (Gong et al., 2019; Liu et al., 2014), reducing vegetation sensitivity to ENSO events in these areas.

This study focuses on China and Australia as representative study areas in the northern and southern hemispheres respectively. Considering the universal influence of ENSO, further research should be conducted in more complex ecosystems and at the global scale. Moreover, the underlying mechanisms of different distribution types of ENSO to climate need to be explored further, providing additional evidence for the long-term influence of ENSO around the globe.

5. CONCLUSIONS

This study characterized the long-term extent, intensity and direction of vegetation responses to ENSO in China and Australia. We explored the underlying mechanisms using climate anomalies in temperature and precipitation as a bridge. We found that where the ENSO develops has a large effect on the intensity and direction of vegetation anomalies for China and Australia, which is induced by opposing controls of CP-type and EP-type ENSO on precipitation and temperature. This study greatly improved our understanding of the mechanisms for vegetation differences in the northern and southern hemispheres during ENSO events and should be extended to global ecosystems in further studies.

ACKNOWLEDGEMENTS

This work was supported by the National Natural Science Foundation of China (42101391), the fellowship of China Postdoctoral Science Foundation (2021M701361) and the Fundamental Research Funds for the Central Universities (CCNU21XJ028).

REFERENCES

Ashok K, Behera S, Rao S, et al. El Niño Modoki and its teleconnection. *Journal of Geophysical Research*, 2007, 112.

Barriopedro D, Gouveia C, Trigo R, et al. The 2009/10 Drought in China: Possible Causes and Impacts on Vegetation. *Journal of Hydrometeorology*, 2012, 13: 1251–1267.

Cai W, Rensch P, Cowan T, et al. Teleconnection Pathways of ENSO and the IOD and the Mechanisms for Impacts on Australian Rainfall. *Journal of Climate*, 2011, 24: 3910-3923.

Collins M, An S I, Cai W, et al. The impact of global warming on the tropical Pacific Ocean and El Niño. *Nature Geoscience*, 2010, 3: 391-397.

Dannenberg M, Song C, Hwang T, et al. Empirical evidence of El Niño–Southern Oscillation influence on land surface phenology and productivity in the western United States. *Remote sensing of Environment*, 2015, 159: 167-180.

Dowdy A J, Climatological Variability of Fire Weather in Australia, *Journal of Applied Meteorology and Climatology*. 2018, 57(2), 221-234.

Feng J, Li J. Influence of El Niño Modoki on spring rainfall over south China. *Journal of Geophysical Research*, 2011, 116: D13102.

Flanagan L B, Adkinson A C. Interacting controls on productivity in a northern Great Plains grassland and implications for response to ENSO events. *Global Change Biology*, 2011, 17(11):3293-3311.

Gong P, Li X, Zhang W. 40-year (1978–2017) human settlement changes in china reflected by impervious surfaces from satellite remote sensing. *Science Bulletin*, 2019, 64: 756-763.

Hao Z, Hao F, Singh VP, et al. Quantifying the relationship between compound dry and hot events and el niño–southern oscillation (enso) at the global scale. *Journal of Hydrology*, 2018, 567: 332-338.

Huang P, Xie S P. Mechanisms of change in enso-induced tropical pacific rainfall variability in a warming climate. *Nature Geoscience*, 2015, 8: 922-926.

Kao H, Yu J. Contrasting Eastern-Pacific and Central-Pacific types of ENSO. *Journal of Climate*, 2009, 22: 615-632.

Kim S T, Yu J Y. The two types of enso in cmip5 models. *Geophysical Research Letters*, 2012, 39: 221-228

Lee T, Mcphaden M J. Increasing intensity of El Niño in the central-equatorial Pacific. *Geophysical Research Letters*. 2010, 37(14): L14603.

Liu D, Wang T, Yang T, et al. Deciphering impacts of climate extremes on tibetan grasslands in the last fifteen years. *Science Bulletin*, 2019, 64: 446.

Liu J, Kuang W, Zhang Z, et al. Spatiotemporal characteristics, patterns and causes of land use changes in China since the late 1980s. *Journal of Geographical Sciences*, 2014, 24: 195-210.

- Lv A, Zhu W, Jia S. Assessment of the sensitivity of vegetation to El-Niño/Southern Oscillation events over China. *Advances in Space Research*, 2012, 50: 1362–1373.
- Ma X, Huete A, Moran S, et al. Abrupt shifts in phenology and vegetation productivity under climate extremes. *Journal of Geophysical Research: Biogeosciences*, 2015, 120: 2036-2052.
- Mariani M, Fletcher M, Holz A, et al. ENSO controls interannual fire activity in southeast Australia. *Geophysical Research Letters*, 2016, 43(20).
- Mccabe G, Ault T, Cook B, et al. Influences of the El Niño Southern Oscillation and the Pacific Decadal Oscillation on the timing of the North American spring. *International Journal of Climatology*, 2012, 32: 2301-2310.
- Mcphaden, M J, Zebiak, S E, Glantz, M H. ENSO as an integrating concept in earth science. *Science*, 2006, 314, 1740.
- Poulter B, Frank D, Ciais P, et al. Contribution of semi-arid ecosystems to interannual variability of the global carbon cycle. *Nature*, 2014, 509: 600.
- Propastin P, Fotso L, Kappas M. Assessment of vegetation vulnerability to ENSO warm events over Africa. *International Journal of Applied Earth Observations & Geoinformation*, 2010, 12:S83-S89.
- Ren H, Jin F. Niño indices for two types of ENSO. *Geophysical Research Letters*, 2011, 38(4): L04704.
- Su Y, Guo Q, Hu T, et al. An updated vegetation map of china (1:1000000). *Science Bulletin*, 2020, 65: 1125.
- Vicente-Serrano S M, Delbart N, Toan L T, et al. El Niño–Southern Oscillation influences on the interannual variability of leaf appearance dates in central Siberia. *Geophysical Research Letters*, 2006, 33.
- Walther G R, Post E, Convey P, et al. Ecological responses to recent climate change. *Nature*, 2002, 416: 389-395.
- Wang B, Luo X, Yang Y M, et al. Historical change of El Niño properties sheds light on future changes of extreme El Niño. *Proceedings of the National Academy of Sciences*, 2019, 116(45):201911130.
- Williamson G J, Prior L D, Jolly W M, et al. Measurement of inter- and intra-annual variability of landscape fire activity at a continental scale: the Australian case. *Environmental Research Letters*. 2016, 11(3): 035003.
- Wu D, Zhao X, Liang S, et al. Time-lag effects of global vegetation responses to climate change. *Global Change Biology*, 2015, 21: 3520-3531.
- Xie Z, Huete A, Cleverly J, et al. Multi-climate mode interactions drive hydrological and vegetation responses to hydroclimatic extremes in Australia. *Remote sensing of Environment*, 2019, 231: 111270.
- Xu L, Samanta A, Costa M H, et al. Widespread decline in greenness of Amazonian vegetation due to the 2010 drought. *Geophysical Research Letters*, 2011, 38: L07402.
- Yang S, Li Z, Yu J Y, et al. El niño-southern oscillation and its impact in the changing climate. *National Science Review*, 2018, 5: 840-857.
- Yeh S W, Kug J S, Dewitte B, et al. El Niño in a changing climate. *Nature*. 2009, 462(7273): 674.
- Yu J, Kao H, Tong L, et al. Subsurface ocean temperature indices for Central-Pacific and Eastern-Pacific types of El Niño and La Niña events. *Theoretical & Applied Climatology*, 2011, 103(3-4):337-344.
- Yu J, Kim S. Transitions between Central-Pacific and Eastern-Pacific Types of ENSO. AGU Fall Meeting Abstracts, 2010: 1277.
- Yuan M, Zhu Q, Zhang J, et al. Global response of terrestrial gross primary productivity to climate extremes. *Science of The Total Environment*. 2020, 750: 142337.
- Zhang A, Jia G, Epstein H, et al. ENSO elicits opposing responses of semi-arid vegetation between Hemispheres. *Scientific Reports*, 2017, 7: 42281.
- Zhang Y, Dannenberg M P, Hwang T, et al. El Niño–Southern Oscillation - induced variability of terrestrial gross primary production during the satellite era. *Journal of Geophysical Research: Biogeosciences*, 2019, 124(8): 2419-2431.
- Zhu Z, Piao S, Myneni R B, et al. Greening of the Earth and its drivers. *Nature Climate Change*, 2016, 6: 791-795.
- Zhu Z, Piao S, Xu Y, et al. The effects of teleconnections on carbon fluxes of global terrestrial ecosystems. *Geophysical Research Letters*, 2017, 44(7): 3209-3218.